Waveform Designs for Joint Radar-Communication Systems with OQAM-OFDM

Qiao Shi[a], Tianxian Zhang*[a], Xianxiang Yu[a], Xinyu Liu[a], Inkyu Lee*[b]

[a]*School of Information and Communication Engineering, University of Electronic Science and Technology of China, Chengdu, Sichuan, P.R. China, 611731*
[b]*School of Electrical Engineering, Korea University, Seoul, South Korea, 02841*
Corresponding authors: Tianxian Zhang and Inkyu Lee
Email: tianxianzhang@gmail.com, inkyu@korea.ac.kr

Abstract

In this paper, we develop a joint radar-communication system with offset quadrature amplitude modulation based orthogonal frequency division multiplexing (OQAM-OFDM), which is capable of realizing the radar and communication functions simultaneously. We first introduce a unified received signal model for the radar and communication systems by taking the multipath effect into account. Then, we propose a method to achieve information demodulation and radar pulse compression at the same time. By analyzing the signal-to-noise ratio (SNR) for the radar operations and the communication individually, we solve an optimization model to maximize the radar SNR and the communication SNR by designing the transmitted sequence of the OQAM-OFDM. Since the optimization problem is NP-hard, we present a joint method involving both the cyclic algorithm and the alternating direction method of multipliers algorithm (CA-ADMM) to obtain a solution. Finally, numerical results verify superior performance of the proposed scheme.

Keywords: Radar-communication system, offset quadrature amplitude modulation based orthogonal frequency division multiplexing (OQAM-OFDM), information demodulation, pulse compression, signal-to-noise ratio (SNR), cyclic algorithm and the alternating direction method of multipliers algorithm (CA-ADMM).

1. Introduction

For the past decades, radar and communication have been developed separately with different goals. The radar is designed to detect and track targets [1, 2], while the communication system mainly focuses on information transmission [3–7]. With the advancement of electronic techniques, a device which employs both radar and communication

functions has been developed for several applications, such as the intelligent transportation systems [8], which need to sense the circumstance and also convey information. As a result, joint radar-communication (RadCom) systems can enjoy advantages of reducing the system weight, size, power consumption, and so on, and have gained lots of interests in recent years [9].

So far, researches on the RadCom system have been divided into two categories: non-simultaneous systems and simultaneous systems [10]. For the non-simultaneous system, the radar and communication functions are operated in different time slots [11]. Although it is quite easy to be implemented, there is a blind spot for radar detection during communication, and it also affects the communication performance. In contrast, the simultaneous system adopts a shared signal, i.e., RadCom signal, which can achieve both the target detection and information transmission functions. Currently, there exist three methods for designing the RadCom signal. First, the radar and communication signals are generated independently and then superimposed [12, 13]. Second, the communication data is modulated on a radar signal [14, 15]. Third, the communication signal is designed, for example, a multi-carrier signal [16, 17]. This method is considered as the most promising one due to its ability for providing high performance in both radar detection and information transmission [17].

In particular, the orthogonal frequency division multiplexing (OFDM) waveform has been employed as a RadCom signal by many studies [17–19]. In [18], the authors analyzed the feasibility of the RadCom system based on the OFDM signal. The work in [19] realized the range detection, synthetic aperture radar (SAR) imaging and communication functions. Additionally, the traditional OFDM scheme based on cyclic prefix (CP) for the RadCom system was proposed in [17, 20–22], which achieves good sidelobe performance for the radar detection and overcomes the multipath effect. However, the presence of CP decreases the spectral efficiency and also wastes a lot of energy. Besides, it is well known that the OFDM signal may suffer from large sidelobes in the frequency domain, which potentially leads to high inter-carrier interference (ICI) and out-of-band radiation [23, 24].

Recently, the offset quadrature amplitude modulation based OFDM (OQAM-OFDM) which does not require CP has been studied as an alternative to the OFDM [24–27]. Normally, a prototype filter [28] with good frequency localization property is applied to the OQAM-OFDM signal to exhibit much lower spectral sidelobes [26]. On this account, the OQAM-OFDM waveform has been considered in several radar systems. The average ambiguity function of the OQAM-OFDM signal was derived in [29–31] which

has a perfect thumbtack shape. In [32], an M-sequence based OQAM-OFDM signal was proposed to improve the signal correlation and the radar range resolution. Also, an approximated inter range cell interference (IRCI)-free pulse compression method using the OQAM-OFDM signal was examined in [34] with low sidelobes. However, all of the aforementioned researches apply the OQAM-OFDM signal to radar applications only without considering the communication functions.

In this paper, we present a system which simultaneously performs the radar and communication functions with the OQAM-OFDM signal. The main contributions of this paper are summarized as follows:

1) A RadCom signal with the OQAM-OFDM is proposed. The traditional OQAM-OFDM signal utilizes the transmitted sequence to carry information, which results in suboptimal performance for the RadCom system. To improve the performance, we introduce a phase term in the OQAM-OFDM signal to transmit information. Then, the transmitted sequence on each subcarrier can be designed to satisfy the radar and communication requirements.

2) A unified received signal model for the RadCom system is presented. Considering each range cell of a radar as a path in communication, the received signal model can be constructed as the convolution of the transmitted signal and the channel response.

3) Focusing on distinct goals for radar and communication, we provide different solving methods and analyze the signal-to-noise ratio (SNR) performance individually. Then, by designing the transmitted sequence of the OQAM-OFDM signal, we propose a joint approach which applies both the cyclic algorithm and the algorithm-alternating direction method of multipliers algorithm (CA-ADMM) to maximize the radar SNR and the communication SNR.

Finally, numerical simulation results are provided to evaluate the effectiveness of the proposed scheme. Simulation results show that our proposed CA-ADMM algorithm can improve both the radar SNR and the communication bit error ratio (BER). Besides, our proposed scheme offers superior performance over the conventional methods.

For the rest of this paper, we first derive the system model in Section 2. Then, the communication demodulation is proposed in Section 3. The radar pulse compression is provided in Section 4. Then, a joint RadCom OQAM-OFDM waveform is designed in Section 5. Numerical simulation results are presented in Section 6. Finally, the conclusions of this paper are drawn in Section 7.

Notation: Boldface lower (upper) case letters represent column vectors (matrices). $\mathbb{C}$, $\mathbb{R}$ and $\mathbb{Z}$ denote the complex, real and integer fields, respectively. $\Im\{\cdot\}$ and $\Re\{\cdot\}$ are,

respectively, the imaginary and real part of complex numbers. The superscripts $(\cdot)^T$, $(\cdot)^*$ and $(\cdot)^H$ indicate transpose, conjugate and conjugate transpose, respectively. E$[\cdot]$ stands for the statistical expectation. $[\mathbf{X}]_{i,j}$ defines the (i,j)th element of a matrix $\mathbf{X}$. $\|\cdot\|_{\mathrm{F}}$ represents the Frobenius matrix norm.

2. System Model

A RadCom system is illustrated in Fig. 1, which can support both radar and communication functions. By transmitting a RadCom signal, we can detect targets by processing the echoes received at the RadCom station. Meanwhile, the communication user receives the RadCom signal and demodulates the transmitted information. In this paper, we introduce a RadCom signal based on the OQAM-OFDM signal. Traditionally, the sequence on each subcarrier of the OQAM-OFDM signal is exploited to carry information in communication systems. In contrast, in our proposed RadCom system, we additionally introduce a phase term in the OQAM-OFDM signal to carry information. Then, we can design the sequence on each subcarrier to optimize the radar and communication performance, which will be discussed later.

Consider an OQAM-OFDM signal with K subcarriers, $2M$ OFDM symbols and length L_s. Denoting the transmitted real sequence on the kth subcarrier as d_k, the proposed OQAM-OFDM RadCom signal at the ith time slot $(i = 0, 1, \ldots, L_s - 1)$ can be written as

$$s_i = \sum_{k=0}^{K-1} \sum_{m=0}^{2M-1} d_k \cos\varphi_{k,m} h\left(i - m\frac{K}{2}\right) e^{j2\pi ki/K}\, e^{j\pi(k+m)/2}, \tag{1}$$

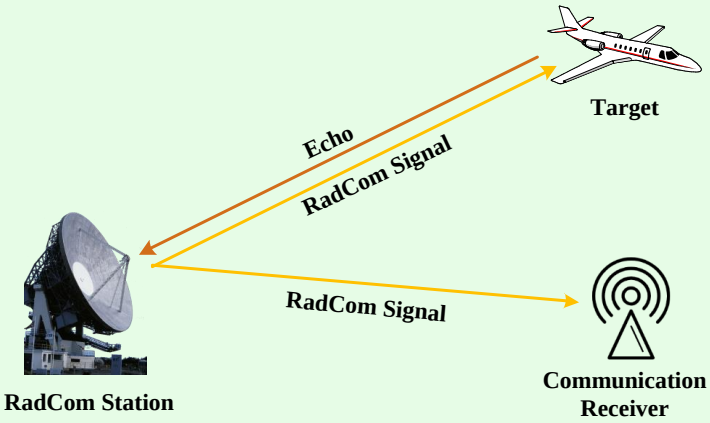

Figure 1 Illustration of the RadCom system.

where $h(i)$ indicates a symmetrical real-valued prototype filter [28], and $\varphi_{k,m}$ can be written as

$$\varphi_{k,m} = \begin{cases} \theta_{k,\frac{m}{2}}, & m \text{ is even} \\ \dfrac{\pi}{2} - \theta_{k,\frac{m-1}{2}}, & m \text{ is odd,} \end{cases} \tag{2}$$

with $\theta_{k,m'}\,(m' = 0, 1, \ldots, M-1)$ being the transmitted information with phase shift keying (PSK) modulation. Thus, the even and odd symbols transmit the real and imaginary part of $e^{j\theta_{k,m'}}$, respectively. As a result, we define the transmitted complex information as

$$c_{k,m'} = d_k(\cos\theta_{k,m'} + j\sin\theta_{k,m'}). \tag{3}$$

For the communication receiver, assuming that the channel impulse response b_r^{com} is known, the received signal ν_i^{com} with length L_ν^{com} can be modeled as [33]

$$\nu_i^{\text{com}} = \sum_{r=0}^{R^{\text{com}}-1} b_r^{\text{com}} s_{i-r} + \omega_i^{\text{com}}, \text{ for } i = 0, 1, \cdots, L_\nu^{\text{com}} - 1, \tag{4}$$

where R^{com} is the length of b_r^{com}, and ω_i^{com} represents the additive white Gaussian noise with zero mean and variance σ_{com}^2 at the receiver. Similarly, for the radar, given the transmitted signal s_i, the received signal ν_i^{rad} at the RadCom station is expressed as [34]

$$\nu_i^{\text{rad}} = \sum_{r=0}^{R^{\text{rad}}-1} b_r^{\text{rad}} s_{i-r} + \omega_i^{\text{rad}}, \text{ for } i = 0, 1, \cdots, L_\nu^{\text{rad}} - 1, \tag{5}$$

where R^{rad} represents the number of range cells and b_r^{rad} denotes the response of scatters within the rth range cell, ω_i^{rad} is the additive white Gaussian noise with zero mean and variance σ_{rad}^2 at the radar, and L_ν^{rad} indicates the length of the received signal.

Note that for communication systems, the receiver demodulates the signal in (4) to estimate $c_{k,m'}$. Meanwhile, for radar systems, to realize the target detection, pulse compression should be operated to improve the SNR, which is equivalent to detecting b_r^{rad} from the received signal in (5). To this end, based on different goals for the radar and communication systems, we separately present the communication demodulation and the radar pulse compression in what follows.

3. Demodulation for communication systems

In this section, we derive a method to acquire the transmitted information from the received signal in (4). First, we demodulate the received signal in (4) as

$$y_{k,m} = \sum_{i=0}^{L_\nu^{\mathrm{com}}-1} \nu_i^{\mathrm{com}} h\left(i - m\frac{K}{2}\right) e^{-j2\pi ki/K}\ e^{-j\pi(k+m)/2}\ . \tag{6}$$

Suppose that the length of the prototype filter L_h is much longer than the maximum delay spread R^{com} of the channel, i.e., $L_h \gg R^{\mathrm{com}}$. On this account, the prototype filter function basically remains unchanged within the delay spread [36].

Then, denoting $\omega_{k,m}$ as the demodulated noise, (6) can be rewritten as [33, 34]

$$y_{k,m} = B_k \left(d_k \cos\varphi_{k,m} + I_{k,m}\right) + \omega_{k,m}, \tag{7}$$

where B_k corresponds to the frequency response of the channel b_r^{com} as

$$B_k = \sum_{r=0}^{R^{\mathrm{com}}-1} b_r^{\mathrm{com}} e^{-j2\pi kr/K}\ , \tag{8}$$

and $I_{k,m}$ represents the interference as

$$I_{k,m} = \sum_{p,q\in\mathbf{\Theta}_{p,q}} d_p \cos\varphi_{p,q} \zeta_{k,m}^{p,q}, \tag{9}$$

with $\mathbf{\Theta}_{p,q} = \{p,q|(p=k\ \ \&\ \ q\neq m), \mathrm{or}\,(\ p\neq k\ \ \&\ \ q\in\mathbb{Z}),\ \mathrm{and}\ |k-p|\leq 1\ \ \&\ \ |m-q|\leq 1\}$, and

$$\zeta_{k,m}^{p,q} = \sum_{i=0}^{L_\nu^{\mathrm{com}}-1} h\left(i - q\frac{K}{2}\right) h\left(i - m\frac{K}{2}\right) e^{j2\pi(p-k)i/K}\ e^{j\pi(p+q-m-k)/2}\ . \tag{10}$$

Here $\zeta_{k,m}^{p,q}$ is an imaginary value for $p,q\in\Theta_{p,q}$ [34], and thus $I_{k,m}$ is also an imaginary value.

Further, we can finally obtain [35]

$$\Re\left\{\frac{y_{k,m}}{B_k}\right\} = d_k\cos\varphi_{k,m} + \Re\left\{\frac{\omega_{k,m}}{B_k}\right\}. \tag{11}$$

Then, we can reconstruct

$$\begin{aligned}\hat{c}_{k,m'} &= \Re\left\{\frac{y_{k,2m'}}{B_k}\right\} + j\Re\left\{\frac{y_{k,2m'+1}}{B_k}\right\} \\ &= c_{k,m'} + \Re\left\{\frac{\omega_{k,2m'}}{B_k}\right\} + j\Re\left\{\frac{\omega_{k,2m'+1}}{B_k}\right\},\ \text{for } m' = 0, 1, \ldots, M-1.\end{aligned} \tag{12}$$

From (12), we can demodulate the transmitted information.

Additionally, to analyze the demodulation performance, we calculate the output SNR for each subcarrier as

$$\mathrm{SNR}_k^{\mathrm{com}} = \frac{d_k^2 |B_k|^2}{\sigma_{\mathrm{com}}^2}, \tag{13}$$

where the noise variance of each subcarrier is $\mathrm{E}\left[\left|\Re\left\{\frac{\omega_{k,2m'}}{B_k}\right\} + j\Re\left\{\frac{\omega_{k,2m'+1}}{B_k}\right\}\right|^2\right] = \frac{\sigma_{\mathrm{com}}^2}{|B_k|^2}$. It is interesting to note that the communication output SNR for each subcarrier is related to the transmitted sequence d_k and the channel frequency response B_k. Thus, we can design d_k to improve $\mathrm{SNR}_k^{\mathrm{com}}$, which will be discussed later.

4. Radar Pulse Compression

In this section, we present a simple and efficient radar pulse compression method. According to (5), we rewrite the radar received signal in vector notation as

$$\mathbf{v} = \mathbf{S}\mathbf{b} + \mathbf{w}, \tag{14}$$

where $\mathbf{v} = \begin{bmatrix} v_0 & v_1 & \cdots & v_{L_\nu^{\mathrm{rad}}-1} \end{bmatrix}^T \in \mathbb{C}^{L_\nu^{\mathrm{rad}}}$ is the received signal vector, $\mathbf{S} \in \mathbb{C}^{L_\nu^{\mathrm{rad}} \times R^{\mathrm{rad}}}$ denotes the transmitted signal matrix, which is given by

$$\mathbf{S} = \begin{pmatrix} s_0 & & 0 \\ \vdots & \ddots & \\ \vdots & & s_0 \\ s_{L_s-1} & & \vdots \\ & \ddots & \vdots \\ 0 & & s_{L_s-1} \end{pmatrix}, \tag{15}$$

$\mathbf{b} = \begin{bmatrix} b_0 & b_1 & \cdots & b_{R^{\mathrm{rad}}-1} \end{bmatrix}^T \in \mathbb{C}^{R^{\mathrm{rad}}}$ indicates the vector corresponding to the range cell, and $\mathbf{w} = \begin{bmatrix} \omega_0 & \omega_1 & \cdots & \omega_{L_\nu^{\mathrm{rad}}-1} \end{bmatrix}^T \in \mathbb{C}^{L_\nu^{\mathrm{rad}}}$ represents the noise vector.

From (15), the columns of $\mathbf{S}$ are linearly independent. Thus, $\mathbf{S}^H\mathbf{S}$ is invertible.

Besides, in practical applications, it is obvious that $L_\nu^{\text{rad}} > R^{\text{rad}}$. Then, the pulse compression can be easily implemented by estimating $\mathbf{b}$ as [37]

$$\hat{\mathbf{b}} = \left(\mathbf{S}^H\mathbf{S}\right)^{-1}\mathbf{S}^H\mathbf{v} = \mathbf{b} + \left(\mathbf{S}^H\mathbf{S}\right)^{-1}\mathbf{S}^H\mathbf{w}. \tag{16}$$

Here, the noise covariance matrix becomes $\mathrm{E}\left[\left(\mathbf{S}^H\mathbf{S}\right)^{-1}\mathbf{S}^H\mathbf{w}\mathbf{w}^H\mathbf{S}\left(\left(\mathbf{S}^H\mathbf{S}\right)^{-1}\right)^H\right] = \sigma_{\text{rad}}^2\left(\mathbf{S}^H\mathbf{S}\right)^{-1}$. In this way, the pulse compression is perfectly realized and there is no interference for the estimate of each range cell from other range cells.

Similarly, we also derive the radar output SNR for the rth range cell as

$$\text{SNR}_r^{\text{rad}} = \frac{\left[\mathbf{b}\mathbf{b}^H\right]_{r,r}}{\sigma_{\text{rad}}^2\left[\left(\mathbf{S}^H\mathbf{S}\right)^{-1}\right]_{r,r}}. \tag{17}$$

In order to achieve the maximum $\text{SNR}_r^{\text{rad}}$, it can be shown that $\mathbf{S}^H\mathbf{S}$ should be diagonal [37]. However, in general, $\mathbf{S}^H\mathbf{S}$ may not be a diagonal matrix. Besides, according to (15), it is obvious that the diagonal elements of $\mathbf{S}^H\mathbf{S}$ are identical to $\|\mathbf{s}\|^2$, where $\mathbf{s} = [s_0\ s_1\ \cdots\ s_{L_s-1}]^T$ is the transmitted signal vector. Also, from (1), $\mathbf{s}$ can be expressed as $\mathbf{s} = \mathbf{\Phi}\mathbf{d}$, where $\mathbf{\Phi}$ is a $L_s \times K$ matrix whose (i,k)th element is given as

$$[\mathbf{\Phi}]_{i,k} = \sum_{m=0}^{2M-1} \cos\varphi_{k,m} h\left(i - m\frac{K}{2}\right) e^{j2\pi ki/K}\, e^{j\pi(k+m)/2}, \tag{18}$$

and $\mathbf{d} = [d_0\ d_1\ \cdots\ d_{K-1}]^T$ denotes the transmitted sequence of the OQAM-OFDM signal. As a result, to maximize the radar $\text{SNR}_r^{\text{rad}}$, we can design $\mathbf{d}$ to make $\mathbf{S}$ satisfy the condition $\mathbf{S}^H\mathbf{S} = \|\mathbf{s}\|^2\mathbf{I}$.

5. Joint optimization for RadCom

Based on the derivations on the RadCom signal in the previous sections, we find that both the radar SNR and communication SNR depend on $\mathbf{d}$. In this section, we develop an optimization model to maximize the radar SNR under the minimum communication SNR constraints, which can be written as

$$\min_{\mathbf{d}} \ \left\|\mathbf{S}^H\mathbf{S} - \mathbf{I}\right\|_{\text{F}}^2 \tag{19}$$

$$\text{s.t. } \mathbf{s} = \mathbf{\Phi}\mathbf{d} \tag{19a}$$

$$\|\mathbf{s}\|^2 = 1 \tag{19b}$$

$$\mathrm{SNR}_k^{\mathrm{com}} \geq \mathrm{SNR}_{\min}, \text{for } k = 0, 1, \ldots, K-1, \tag{19c}$$

where the constraint (19b) denotes the energy constraint for the transmitted signal, and the $\mathrm{SNR}_{\min}$ represents the communication minimum output SNR to obtain an acceptable BER. Therefore, by solving problem (19), we not only maximize the radar SNR performance but also guarantee the communication SNR performance.

From (19), it is not easy to directly acquire the optimal solution for $\mathbf{d}$. Thus, we propose a CA-ADMM algorithm to solve the problem (19). Note that the objective of (19) is a quartic function of $\mathbf{S}$, which is difficult to tackle. On this account, adopting a similar approach in [38, 39], we replace the objective of (19) as

$$\begin{aligned} &\min_{\mathbf{S},\mathbf{Q}} \ \|\mathbf{S}-\mathbf{Q}\|_{\mathrm{F}}^2 \\ &\text{s.t. } \mathbf{Q}^H\mathbf{Q} = \mathbf{I}, \end{aligned} \tag{20}$$

where $\mathbf{Q}$ is a $L_\nu^{\mathrm{rad}} \times R^{\mathrm{rad}}$ semi-unitary matrix. Then, we can solve the problem (20) by using the CA algorithm [38].

Let us denote

$$\mathbf{S}^H = \mathbf{U}\mathbf{\Sigma}\mathbf{V}^H \tag{21}$$

as the singular value decomposition (SVD) of $\mathbf{S}^H$, where $\mathbf{U} \in \mathbb{C}^{R^{\mathrm{rad}} \times R^{\mathrm{rad}}}$ is a unitary matrix, $\mathbf{\Sigma} \in \mathbb{R}^{R^{\mathrm{rad}} \times R^{\mathrm{rad}}}$ represents a diagonal matrix, and $\mathbf{V} \in \mathbb{C}^{L_v^{\mathrm{rad}} \times R^{\mathrm{rad}}}$ indicates a semi-unitary matrix. Then, for a given $\mathbf{S}$, a solution of (20) can be given as

$$\hat{\mathbf{Q}} = \mathbf{V}\mathbf{U}^H. \tag{22}$$

Therefore, based on (15), the problem (20) can be converted to

$$\begin{aligned} &\min_{\mathbf{s}} \ \sum_{r=0}^{R^{\mathrm{rad}}-1} \|\mathbf{s}-\mathbf{q}_r\|^2 \\ &\text{s.t. } \|\mathbf{s}\|^2 = 1, \end{aligned} \tag{23}$$

where $\mathbf{q}_r \in \mathbb{C}^{L_s \times 1}$ is the subvector of the rth column of $\hat{\mathbf{Q}}$, whose position is the same as that of $\mathbf{s}$ in the rth column of $\mathbf{S}$. Thus, the final optimization model for optimizing

$\mathbf{d}$ can be constructed as

$$\begin{aligned} &\min_{\mathbf{d}} \sum_{r=0}^{R^{\text{rad}}-1} \|\mathbf{\Phi d}-\mathbf{q}_r\|^2 \\ &\text{s.t. (19a)-(19c).} \end{aligned} \tag{24}$$

The problem (24) is in general a NP-hard problem because of the non-convexity of the constraints [40, 41]. Thus, we introduce the ADMM algorithm [42] to obtain a solution of (24). First, we develop the augmented Lagrangian as

$$L\left(\mathbf{s},\mathbf{d},\boldsymbol{\lambda}\right)=\sum_{r=0}^{R^{\text{rad}}-1}\|\mathbf{\Phi d}-\mathbf{q}_r\|^2+\Re\left\{\boldsymbol{\lambda}^H\left(\mathbf{s}-\mathbf{\Phi d}\right)\right\}+\frac{\alpha}{2}\|\mathbf{s}-\mathbf{\Phi d}\|^2, \tag{25}$$

where $\boldsymbol{\lambda}$ is the multiplier vector of length L_s, and α represents the penalty factor. Then, the ADMM algorithm can be exploited to determine $(\mathbf{s},\mathbf{d},\boldsymbol{\lambda})$ in an alternating fashion to minimize $L\left(\mathbf{s},\mathbf{d},\boldsymbol{\lambda}\right)$ by accounting for the constraints in problem (24).

Let us denote $\mathbf{s}^{(t)},\mathbf{d}^{(t)},\boldsymbol{\lambda}^{(t)},\mathbf{q}_r^{(t)}$ as the t-th iteration values of $\mathbf{s},\mathbf{d},\boldsymbol{\lambda},\mathbf{q}_r$, respectively. $\mathbf{q}_r^{(t+1)}$ can be determined by (22) with $\mathbf{s}^{(t)}$. Additionally, we can update $\mathbf{s},\mathbf{d},\boldsymbol{\lambda}$ by

$$\begin{aligned} \mathbf{s}^{(t+1)}&=\arg\min_{\mathbf{s}\in\Theta_{\mathbf{s}}} L\left(\mathbf{s},\mathbf{d}^{(t)},\boldsymbol{\lambda}^{(t)}\right)\\ \mathbf{d}^{(t+1)}&=\arg\min_{\mathbf{d}\in\Theta_{\mathbf{d}}} L\left(\mathbf{s}^{(t+1)},\mathbf{d},\boldsymbol{\lambda}^{(t)}\right) \end{aligned} \tag{26}$$

$$\boldsymbol{\lambda}^{(t+1)}=\boldsymbol{\lambda}^{(t)}+\alpha\left(\mathbf{s}^{(t+1)}-\mathbf{\Phi d}^{(t+1)}\right), \tag{27}$$

where $\Theta_{\mathbf{s}}=\{\mathbf{s}|\,\|\mathbf{s}\|^2=1\}$, $\Theta_{\mathbf{d}}=\left\{\mathbf{d}|\mathbf{d}\in\mathbb{R}^K,|d_k|\geq\rho_k,\forall k\right\}$ with $\rho_k=\sqrt{\frac{\sigma_{\text{com}}^2\text{SNR}_{\min}}{|B_k|^2}}$. The detailed procedures to solve $\mathbf{s}^{(t+1)}$ and $\mathbf{d}^{(t+1)}$ are given as follows:

5.1. Update of $\mathbf{s}$ *with given* $\mathbf{d}^{(t)},\boldsymbol{\lambda}^{(t)},\mathbf{q}_r^{(t+1)}$

Ignoring the constant terms, the subproblem with respect to $\mathbf{s}$ can be written as

$$\begin{aligned} &\min_{\mathbf{s}} \Re\left\{\boldsymbol{\lambda}^{(t)H}\left(\mathbf{s}-\mathbf{\Phi d}^{(t)}\right)\right\}+\tfrac{\alpha}{2}\|\,\mathbf{s}-\mathbf{\Phi d}^{(t)}\,\|^2\\ &\text{s.t. } \|\mathbf{s}\|^2=1, \end{aligned} \tag{28}$$

which can be simplified as

$$\begin{aligned} &\min_{\mathbf{s}} \text{Re}\left\{\mathbf{x}^H\mathbf{s}\right\}\\ &\text{s.t. } \|\mathbf{s}\|^2=1, \end{aligned} \tag{29}$$

where $\mathbf{x} = \boldsymbol{\lambda}^{(t)} - \alpha^H \boldsymbol{\Phi}\mathbf{d}^{(t)}$. Then, we can obtain a close-form solution as

$$\mathbf{s}^{(t+1)} = -\frac{\mathbf{x}}{\|\mathbf{x}\|}. \tag{30}$$

5.2. Update of $\mathbf{d}$ *with given* $\mathbf{s}^{(t+1)}, \boldsymbol{\lambda}^{(t)}$, $\mathbf{q}_r^{(t+1)}$

The subproblem including the terms dependent on $\mathbf{d}$ is given by

$$\begin{aligned} &\min_{\mathbf{d}} \sum_{r=0}^{R^{\text{rad}}-1} \left\| \boldsymbol{\Phi}\mathbf{d} - \mathbf{q}_r^{(t+1)} \right\|^2 + \Re\left\{ \boldsymbol{\lambda}^{(t)H} \left(\mathbf{s}^{(t+1)} - \boldsymbol{\Phi}\mathbf{d} \right) \right\} + \tfrac{\alpha}{2} \| \mathbf{s}^{(t+1)} - \boldsymbol{\Phi}\mathbf{d} \|^2 \\ &\text{s.t.} \quad |d_k| \geq \rho_k, \forall k. \end{aligned} \tag{31}$$

Then, the problem in (31) can be expressed as

$$\begin{aligned} &\min_{\mathbf{d}} \ \mathbf{d}^H \boldsymbol{\Omega}\mathbf{d} - \text{Re}\left\{ \mathbf{d}^H \mathbf{y} \right\} \\ &\text{s.t.} \quad |d_k| \geq \rho_k, \forall k, \end{aligned} \tag{32}$$

where $\boldsymbol{\Omega} = \left(1 + \frac{\alpha}{2}\right) \boldsymbol{\Phi}^H \boldsymbol{\Phi}$ and $\mathbf{y} = \boldsymbol{\Phi}^H \left(2 \sum_{r=1}^{R^{\text{rad}}} \mathbf{q}_r^{(t+1)} + \boldsymbol{\lambda}^{(t)} + \alpha \mathbf{s}^{(t+1)} \right)$. The problem (32) can be addressed by the coordinate descent (CD) algorithm [43, 44]. For updating d_k, we keep all the other elements of $\mathbf{d}$ as fixed, and we solve

$$\begin{aligned} &\min_{d_k} \ a_1 d_k^2 + a_2 d_k + a_3 \\ &\text{s.t.} \quad |d_k| \geq \rho_k, \end{aligned} \tag{33}$$

where a_1, a_2 and a_3 are defined as $a_1 = [\boldsymbol{\Omega}]_{k,k}$,

$$a_2 = 2 \sum_{\substack{l=0 \\ l \neq k}}^{K-1} \Re\left\{ [\boldsymbol{\Omega}]_{l,k} \right\} d_l - \Re\left\{ y_k \right\}, \tag{34}$$

$$a_3 = \sum_{\substack{l=0 \\ l \neq k}}^{K-1} \sum_{\substack{e=0 \\ e \neq k}}^{K-1} [\boldsymbol{\Omega}]_{l,e} d_l d_e - \sum_{\substack{l=0 \\ l \neq k}}^{K-1} \Re\left\{ y_l \right\} d_l. \tag{35}$$

Algorithm 1: CA-ADMM Algorithm for solving (19)

Set $t = 0$, and initialize $\mathbf{s}^{(0)}$, $\mathbf{d}^{(0)}$, $\boldsymbol{\lambda}^{(0)}$, $\mathbf{q}_r^{(0)}$, α, and $\mathrm{SNR}_{\min}$
repeat
  Find $\mathbf{q}_r^{(t+1)}$ by solving (22)
  Update $\mathbf{s}^{(t+1)}$ by solving (30)
  for $k = 0$ to $K-1$ **do**
    Find $d_k^{(t+1)}$ by solving (36) and update $\mathbf{d}^{(t+1)}$
  end for
  Update $\boldsymbol{\lambda}^{(t+1)}$ by (27)
  Update $t \leftarrow t+1$
until convergence

Therefore, we can obtain a solution for d_k as

$$d_k^{(t+1)} = \begin{cases} -\dfrac{a_2}{2a_1}, & \text{if } \left|\dfrac{a_2}{2a_1}\right| \geq \rho_k \\ \rho_k, & \text{if } 0 \leq -\dfrac{a_2}{2a_1} < \rho_k \\ -\rho_k, & \text{else.} \end{cases} \tag{36}$$

We continue the above procedures until all elements of $\mathbf{d}^{(t)}$ are updated. Then, we finally acquire $\mathbf{d}^{(t+1)}$.

The proposed CA-ADMM algorithm for problem (19) is summarized in Algorithm 1, where the main computational complexity is related to the number of range cells R^{rad} and the number of iterations. For each iteration, the main computational complexity corresponds to the SVD when updating $\mathbf{q}_r$. As a result, the proposed CA-ADMM algorithm requires a computational complexity of $O(F(R^{\mathrm{rad}})^3)$, where F denotes the number of iterations.

6. Numerical Results

This section is provided to assess the proposed CA-ADMM based RadCom design method. We set the number of subcarriers as $K = 128$, the number of symbols as $2M = 4$, the number of range cells as $R^{\mathrm{rad}} = 64$, and the channel length as $R^{\mathrm{com}} = 6$ with the power profile (in dB) $\{-6.0, 0.0, -7.0, -22.0, -16.0, -20.0\}$ and the corresponding delay profile (in μs) $\{-3, 0, 2, 4, 7, 11\}$. We use the binary phase shift keying (BPSK) modulation scheme. The raised cosine filter is utilized as the prototype filter of the OQAM-OFDM signal. $\mathbf{d}$ and $\boldsymbol{\lambda}$ are initialized randomly. All simulation results are

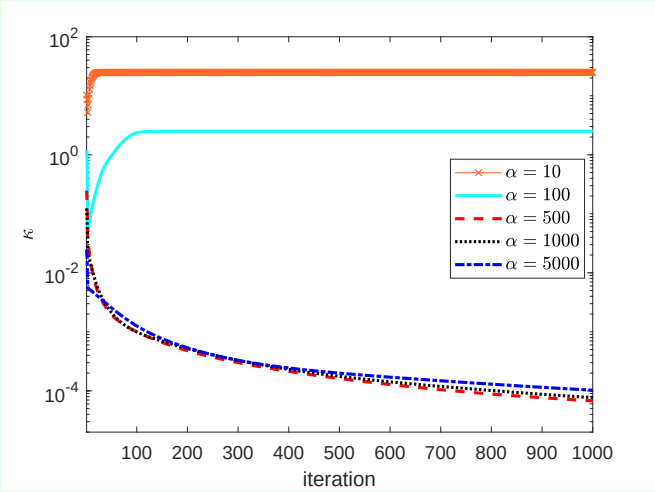

Figure 2 Residual κ with respect to iterations with different values of α.

obtained under the Monte Carlo experiments with 100 experiments.

In Algorithm 1, the penalty factor α and the required minimum communication output $\mathrm{SNR}_{\mathrm{min}}$ affect the performance of the proposed method. To verify the effect, Fig. 2 displays the residual $\kappa^{(t)} = \max\left\{\|\mathbf{s}^{(t)} - \mathbf{\Phi}\mathbf{d}^{(t)}\|, \|\mathbf{d}^{(t)} - \mathbf{d}^{(t-1)}\|\right\}$ against iterations with respect to different α with $\mathrm{SNR}_{\mathrm{min}} = -30\,\mathrm{dB}$ and the input SNR 0 dB. Herein, the convergence threshold is set as 10^{-4} for the CA-ADMM algorithm [42, 45]. From Fig. 2, when α is small, such as $\alpha = 10, 100$, the proposed algorithm cannot guarantee convergence. With a larger α, the convergence can be ensured. As a consequence, a larger α should be chosen.

In Fig. 3, with the input SNR of 0 dB and $\mathrm{SNR}_{\mathrm{min}} = -30\,\mathrm{dB}$, we present the radar output SNR and the integrated sidelobe ratio (ISLR) curves with respect to iterations. It is seen that the radar output SNR grows gradually with iterations and finally converges to $\mathrm{SNR}_{\mathrm{max}}$, which is the maximum attainable SNR. $\mathrm{SNR}_{\mathrm{max}}$ is computed as the length of the transmitted signal. Also, with the increasing iterations, the ISLR decreases and quickly converges. The proposed algorithm realizes a gain of 4.35 dB for the output SNR and 3.73 dB for the ISLR, compared to the no iteration case. Meanwhile, we can find that a smaller α achieves a fast convergence.

In addition, with the input SNR of 10 dB and $\mathrm{SNR}_{\mathrm{min}} = -30\,\mathrm{dB}$, the communication BER curves which are obtained with the Monte Carlo experiments are shown in Fig. 4. Similarly, we can see that the BER performance is improved with iterations. Therefore, we can conclude that we first need to choose an appropriate value for α to ensure convergence and make the algorithm converge as soon as possible. we set $\alpha = 500$ in

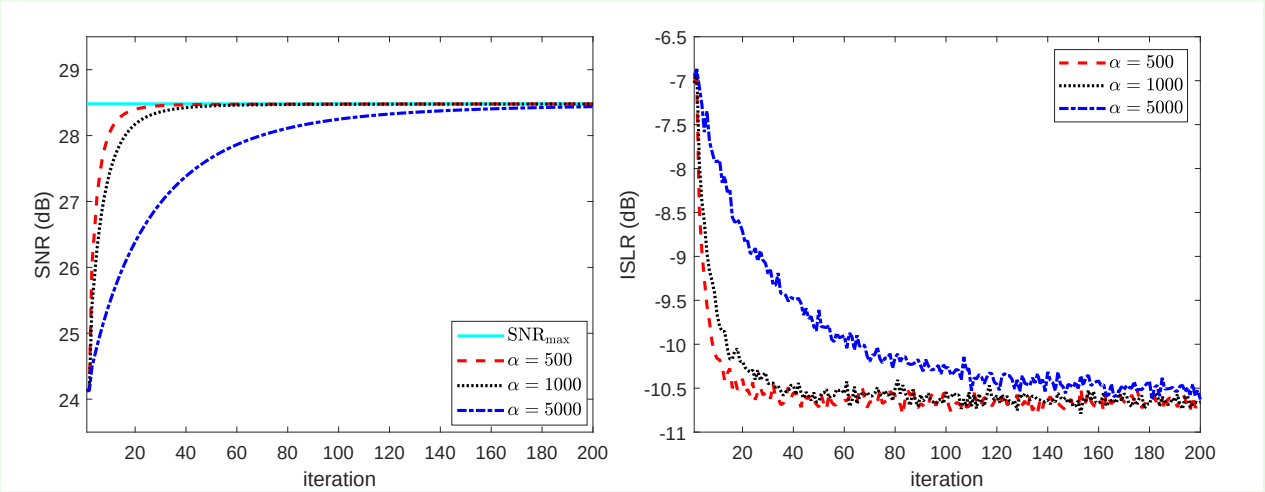

(a) (b)

Figure 3 Radar performance with respect to iterations with different values of α (a) Output SNR (b) ISLR.

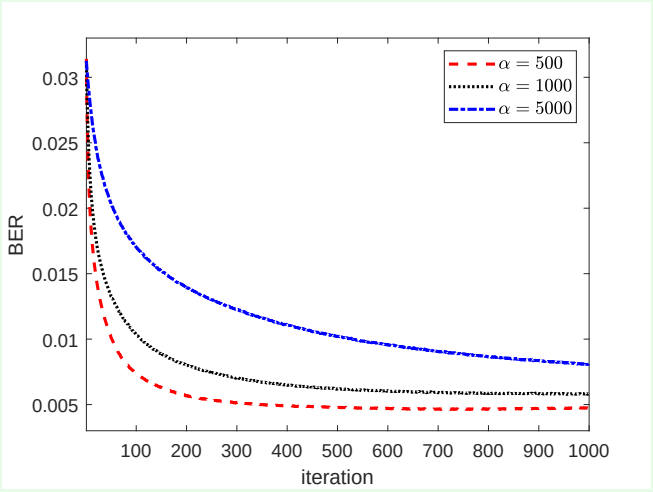

Figure 4 Communication BER curves with respect to iterations with different values of α.

the following simulations. Further, from these plots, we confirm that the performance improvement is achieved for both the radar and communication.

Next, we analyze the effect brought by SNR_{min}. The residual κ with respect to iterations is depicted in Fig. 5 with different SNR_{min} and the input SNR of 0 dB. As expected, we can check that the proposed algorithm gradually converges with iterations when SNR_{min} is not greater than the input SNR. It takes less time for a larger value of SNR_{min} to converge, but the algorithm cannot converge when SNR_{min} is too large. The reason is a larger SNR_{min} means a stronger communication constraint, resulting in the

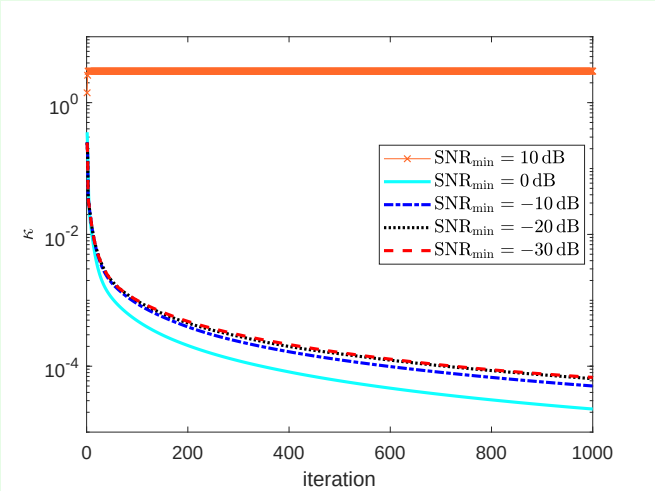

Figure 5 Residual κ with respect to iterations with different values of $\mathrm{SNR}_{\min}$.

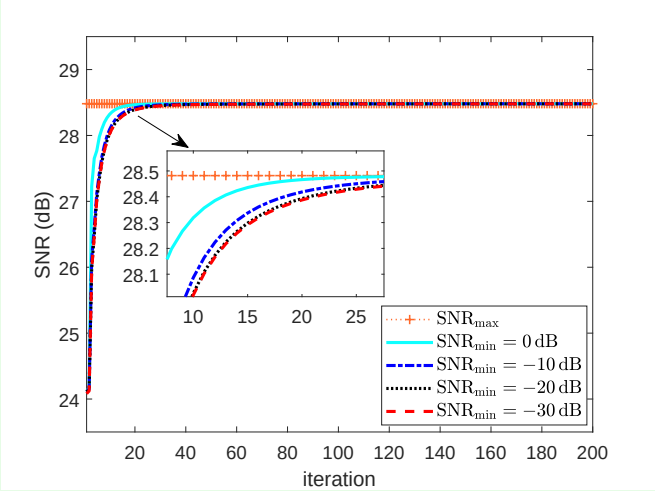

Figure 6 Radar SNR with respect to iterations with different values of $\mathrm{SNR}_{\min}$.

reduced size of the feasible set.

In Fig. 6 and Fig. 7, the radar and communication simulation results with different $\mathrm{SNR}_{\min}$ are demonstrated, respectively. The input SNR for radar is 0 dB and 10 dB for communication. From Fig. 6, as can be seen, $\mathrm{SNR}_{\min}$ has little influence on the radar performance, and all the results quickly converge to $\mathrm{SNR}_{\max}$. In Fig. 7, a larger $\mathrm{SNR}_{\min}$ results in better BER performance. To this end, when choosing $\mathrm{SNR}_{\min}$, we can let it be equal to the input SNR, which ont only can maximize the radar output SNR but also greatly promote the communication performance.

In Fig. 8 and Fig. 9, we further analyze the radar and communication performance with different input SNR for the case where $\mathrm{SNR}_{\min}$ is set to the input SNR. The

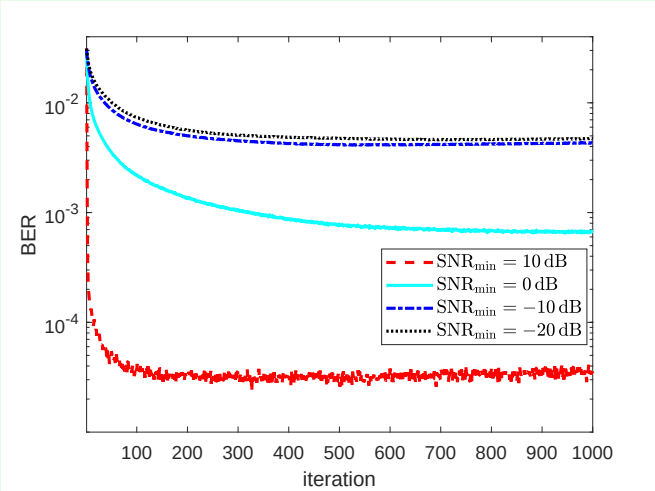

Figure 7 Communication BER with respect to iterations with different values of $\mathrm{SNR}_{\min}$.

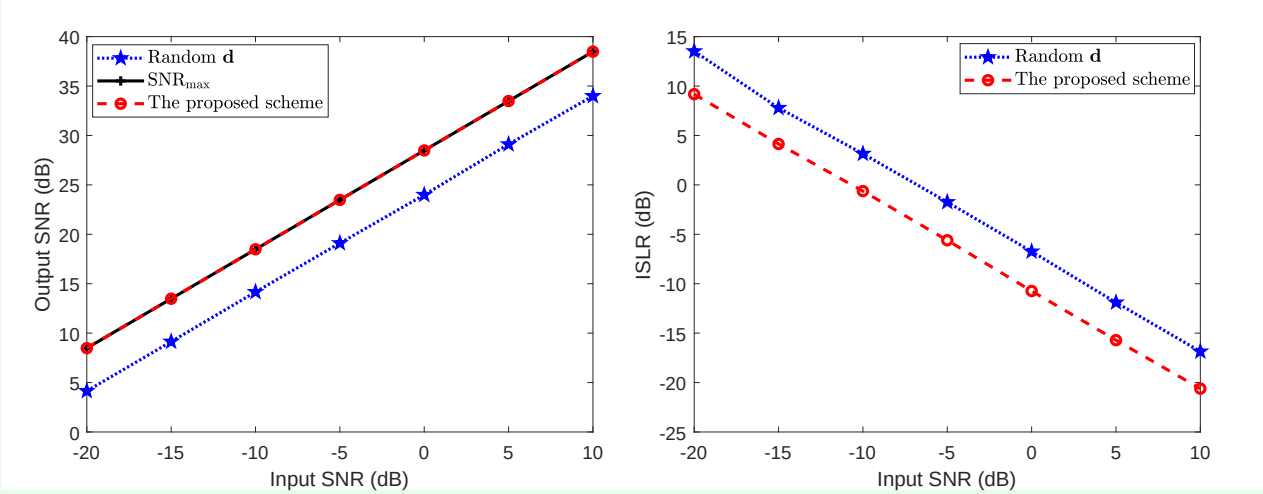

(a) (b)

Figure 8 Radar simulation results with respect to input SNR. (a) Ouput SNR (b) ISLR

results with randomly generated **d** are given as benchmarks for comparison. In Fig. 8, the proposed algorithm can always reach the maximum SNR, and both the output SNR and ISLR performance outperform the traditional scheme. Compared with the conventional scheme, the proposed algorithm achieves an output SNR gain of 4.43 dB and ISLR gain of 2.99 dB. Fig. 9 illustrates the communication BER simulation results. With the increased input SNR, the proposed algorithm achieves large performance gains compared with the conventional scheme. From the above simulation results, we verify the effectiveness of the proposed scheme. The proposed scheme displays superior radar and communication performance compared with the conventional methods.

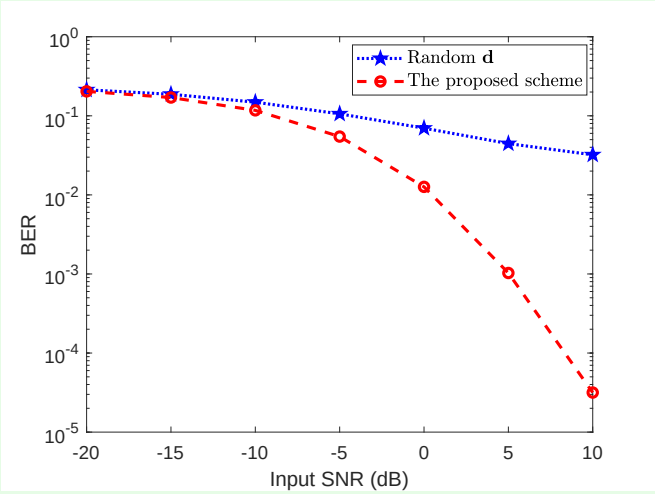

Figure 9 Communication BER results with respect to input SNR.

7. conclusion

In this paper, a joint RadCom OQAM-OFDM system has been proposed, which simultaneously realizes the communication and radar pulse compression. A unified received signal model for the radar and communication systems has been constructed. To satisfy the goals of radar and the communication, we provide different methods to solve the problem. We then have analyzed the output SNR, and found that both the radar SNR and communication SNR are related to the transmitted sequence of the OQAM-OFDM signal. As a result, by designing the transmitted sequence, an optimization model has been established to maximize the radar SNR and also ensure the minimum communication SNR. We have employed the CA algorithm to transform the problem into a quadratic problem, and then solve it under the framework of the ADMM algorithm. Finally, the effectiveness of the proposed scheme has been validated via numerical simulation results. The proposed scheme displays superior radar SNR, sidelobe performance and the BER performance over the conventional schemes.

8. Acknowledgment

This work was supported in part by the National Natural Science Foundation of China under Grant 61971109, in part by the Chang Jiang Scholars Program, the GF Science and Technology Special Innovation Zone Project, and in part by the Fundamental Research Funds of Central Universities under Grant 2672018ZYGX2018J009.

References

[1] J. Marcum, "A statistical theory of target detection by pulsed radar," *IRE Transactions on Information Theory*, vol. 6, no. 2, pp. 59-267, Apr. 1960.

[2] W. Yi, Y. Yuan, R. Hoseinnezhad and L. Kong, "Resource scheduling for distributed multi-target tracking in netted colocated MIMO radar systems," *IEEE Transactions on Signal Processing*, vol. 68, pp. 1602-1617, Feb. 2020.

[3] D. Chen and J. N. Laneman, "Modulation and demodulation for cooperative diversity in wireless systems," *IEEE Transactions on Wireless Communications*, vol. 5, no. 7, pp. 1785-1794, Jul. 2006.

[4] H. Kim, H. Lee, M. Ahn, H. Kong and I. Lee, "Joint subcarrier and power allocation methods in full duplex wireless powered communication networks for OFDM systems," *IEEE Transactions on Wireless Communications*, vol. 15, no. 7, pp. 4745-4753, Jul. 2016.

[5] H. Kong, C. Song, M. Ahn and I. Lee, "Diversity of coded beamforming in MIMO-OFDM AF relaying systems with direct link," *IEEE Transactions on Vehicular Technology*, vol. 64, no. 8, pp. 3817-3822, Aug. 2015.

[6] K. Lee, J. Kim, J. Jung and I. Lee, "Zadoff-Chu sequence based signature identification for OFDM," *IEEE Transactions on Wireless Communications*, vol. 12, no. 10, pp. 4932-4942, Oct. 2013.

[7] K. Lee, S. Moon, S. Kim and I. Lee, "Sequence designs for robust consistent frequency-offset estimation in OFDM systems," *IEEE Transactions on Vehicular Technology*, vol. 62, no. 3, pp. 1389-1394, Mar. 2013.

[8] G. Dimitrakopoulos and P. Demestichas, "Intelligent transportation systems," *IEEE Vehicular Technology Magazine*, vol. 5, no. 1, pp. 77-84, Mar. 2010.

[9] S. H. Dokhanchi, B. S. Mysore, K. V. Mishra and B. Ottersten, "A mmWave automotive joint radar-communications system," *IEEE Transactions on Aerospace and Electronic Systems*, vol. 55, no. 3, pp. 1241-1260, Jun. 2019.

[10] P. Kumari, J. Choi, N. Gonzalez-Prelcic and R. W. Heath, "IEEE 802.11ad-based radar: an approach to joint vehicular communication-radar system," *IEEE Transactions on Vehicular Technology*, vol. 67, no. 4, pp. 3012-3027, Apr. 2018.

[11] H. Zhang, L. Li and K. Wu, "24GHz software-defined radar system for automotive applications," *in Proc. European Conference on Wireless Technologies*, Munich, Germany, pp. 138-141, Dec. 2007.

[12] M. Roberton and E. R. Brown, "Integrated radar and communications based on chirped spread-spectrum techniques," *in Proc. IEEE MTT-S International Microwave Symposium Digest*, Philadelphia, USA, pp. 611-614, Jul. 2003.

[13] M. Jamil, H. Zepernick and M. I. Pettersson, "On integrated radar and communication systems using Oppermann sequences," *in Proc. IEEE Military Communications Conference*, San Diego, USA, pp. 1-6, Nov. 2008.

[14] M. Nowak, M. Wicks, Z. Zhang and Z. Wu, "Co-designed radar-communication using linear frequency modulation waveform," *IEEE Aerospace and Electronic Systems Magazine*, vol. 31, no. 10, pp. 28-35, Oct. 2016.

[15] Q. Li, K. Dai, Y. Zhang and H. Zhang, "Integrated waveform for a joint radar-communication system with high-speed transmission," *IEEE Wireless Communications Letters*, vol. 8, no. 4, pp. 1208-1211, Aug. 2019.

[16] C. R. Berger, B. Demissie, J. Heckenbach, P. Willett and S. Zhou, "Signal processing for passive radar using OFDM waveforms," *IEEE Journal of Selected Topics in Signal Processing*, vol. 4, no. 1, pp. 226-238, Feb. 2010.

[17] C. Sturm and W. Wiesbeck, "Waveform design and signal processing aspects for fusion of wireless communications and radar sensing," *IEEE Proceedings*, vol. 99, no. 7, pp. 1236-1259, Jul. 2011.

[18] C. Sturm, T. Zwick and W. Wiesbeck, "An OFDM system concept for joint radar and communications operations," *in Proc. IEEE Vehicular Technology Conference*, Barcelona, Spain, pp. 1-5, Apr. 2009.

[19] D. Garmatyuk, J. Schuerger and K. Kauffman, "Multifunctional software-defined radar sensor and data communication system," *IEEE Sensors Journal*, vol. 11, no. 1, pp. 99-106, Jan. 2011.

[20] T. Zhang, X. Xia and L. Kong, "IRCI free range reconstruction for SAR imaging with arbitrary length OFDM pulse," *IEEE Transactions on Signal Processing*, vol. 62, no. 18, pp. 4748-4759, Sep. 2014.

[21] T. Zhang and X. Xia, "OFDM synthetic aperture radar imaging with sufficient cyclic prefix," *IEEE Transactions on Geoscience and Remote Sensing*, vol. 53, no. 1, pp. 394-404, Jan. 2015.

[22] X. Xia, T. Zhang and L. Kong, "MIMO OFDM radar IRCI free range reconstruction with sufficient cyclic prefix," *IEEE Transactions on Aerospace and Electronic Systems*, vol. 51, no. 3, pp. 2276-2293, Jul. 2015.

[23] D. Zhang, M. Matthe, L. L. Mendes and G. Fettweis, "A study on the link level performance of advanced multicarrier waveforms under MIMO wireless communication channels," *IEEE Transactions on Wireless Communications*, vol. 16, no. 4, pp. 2350-2365, Apr. 2017.

[24] R. Zakaria and D. Le Ruyet, "A novel filter-bank multicarrier scheme to mitigate the intrinsic interference: application to MIMO systems," *IEEE Transactions on Wireless Communications*, vol. 11, no. 3, pp. 1112-1123, Mar. 2012.

[25] T. Fusco and M. Tanda, "Blind frequency-offset estimation for OFDM/OQAM systems," *IEEE Transactions on Signal Processing*, vol. 55, no. 5, pp. 1828-1838, May 2007.

[26] T. Ihalainen, A. Ikhlef, J. Louveaux and M. Renfors, "Channel equalization for multi-antenna FBMC/OQAM receivers," *IEEE Transactions on Vehicular Technology*, vol. 60, no. 5, pp. 2070-2085, Jun. 2011.

[27] D. Katselis, E. Kofidis, A. Rontogiannis and S. Theodoridis, "Preamble-based channel estimation for CP-OFDM and OFDM/OQAM systems: A comparative study," *IEEE Transactions on Signal Processing*, vol. 58, no. 5, pp. 2911-2916, May 2010.

[28] M. Bellanger, "FBMC physical layer: A primer," *PHYDYAS*, 2010.

[29] W. Cao, J. Zhu, X. Li, W. Hu and J. Lei, "Feasibility of multi-carrier modulation signals as new illuminators of opportunity for passive radar: orthogonal frequency division multiplexing versus filter-bank multi-carrier," *IET Radar, Sonar and Navigation*, vol. 10, no. 6, pp. 1080-1087, Jun. 2016.

[30] W. Cao, L. Zhang, W. Hu, J. Lei and X. Du, "OFDM ambiguity function improvement with FBMC prototype filter for passive radar," *in Proc. International Radar Symposium*, Prague, pp. 1-9, Jun. 2017.

[31] M. Liu, J. Zhang and B. Li, "Feasibility analysis of OFDM/OQAM signals as illuminator of opportunity for passive detection," *in Proc. IEEE International Conference on Signal Processing*, Beijing, China, pp. 793-796, Aug. 2018.

[32] W. Xu, C. Wang, G. Cui, W. Wang and Y. Zhang, "The M-sequence encoding method for radar-communication system based on filter bank multi-carrier," *in Proc. International Conference on Advanced Infocomm Technology*, Chengdu, China, pp. 255-259, Nov. 2017.

[33] D. Kong, X. Zheng, Y. Zhang and T. Jiang, "Frame repetition: A solution to imaginary interference cancellation in FBMC/OQAM systems," *IEEE Transactions on Signal Processing*, vol. 68, pp. 1259-1273, Feb. 2020.

[34] Q. Shi, X. Li, T. Zhang, G. Cui and L. Kong, "OQAM-OFDM radar approximated IRCI-Free pulse compression," *IEEE Transactions on Vehicular Technology*, vol. 69, no. 9, pp. 10009-10018, Sep. 2020.

[35] T. Jiang, D. Chen, C. Ni, and D. Qu, "OQAM/FBMC for Future Wireless Communications: Principles, Technologies and Applications," Cambridge, MA, USA: Elsevier, 2017.

[36] E. Kofidis, "Preamble-based estimation of highly frequency selective channels in FBMC/OQAM systems," *IEEE Transactions on Signal Processing*, vol. 65, no. 7, pp. 1855-1868, Apr. 2017.

[37] S. M. Kay, "Fundamentals of statistical signal processing," *Technometrics*, 1993.

[38] P. Stoica, J. Li and X. Zhu, "Waveform synthesis for diversity-based transmit beampattern design," *IEEE Transactions on Signal Processing*, vol. 56, no. 6, pp. 2593-2598, Jun. 2008.

[39] J. Li, P. Stoica and X. Zheng, "Signal synthesis and receiver design for MIMO radar imaging," *IEEE Transactions on Signal Processing*, vol. 56, no. 8, pp. 3959-3968, Aug. 2008.

[40] S. Boyd and L. Vandenberghe, "Convex optimization", *Cambridge University Press*, 2004.

[41] X. Yu, G. Cui, J. Yang and L. Kong, "Wideband MIMO radar beampattern shaping with space-frequency nulling", *Signal Processing*, Vol. 160, pp. 80-87, Jul. 2019.

[42] S. Boyd, N. Parikh, E. Chu, B. Peleato and J. Eckstein, "Distributed optimization and statistical learning via the alternating direction method of multipliers," *Found and Trends in Machine Learning*, vol. 3, no. 1, pp. 1-122, 2011.

[43] X. Yu, G. Cui, L. Kong, J. Li and G. Gui, "Constrained waveform design for colocated MIMO radar with uncertain steering matrices," *IEEE Transactions on Aerospace and Electronic Systems*, vol. 55, no. 1, pp. 356-370, Feb. 2019.

[44] M. A. Kerahroodi, A. Aubry, A. De Maio, M. M. Naghsh and M. Modarres-Hashemi, "A coordinate-descent framework to design low PSL/ISL sequences," *IEEE Transactions on Signal Processing*, vol. 65, no. 22, pp. 5942-5956, Nov. 2017.

[45] X. Yu, G. Cui, J. Yang and L. Kong, "MIMO radar transmit-receive design for moving target detection in signal-dependent clutter," *IEEE Transactions on Vehicular Technology*, vol. 69, no. 1, pp. 522-536, Jan. 2020.